OKU Fen Bilimleri Enstitüsü Dergisi
7(3): 1319-1341, 2024

OKU Journal of The Institute of Science and Technology, 7(3): 1319-1341, 2024

Osmaniye Korkut Ata Üniversitesi Fen Bilimleri Enstitüsü Dergisi

Osmaniye Korkut Ata University Journal of The Institute of Science and Technology

Green Synthesis of Chitosan-Coated Silver Nanoparticles (Ch-AgNPs): Harnessing Nature for Sustainable and Safe Nanomaterial Production

Asli KARA[1*], Burcin OZCELIK[2]

[1,2]Hitit University, Faculty of Art and Science, Molecular Biology and Genetic Department, 19100, Corum

[1]https://orcid.org/0000-0002-0347-0222
[2]https://orcid.org/0000-0003-0115-4194
*Corresponding author: aslicapli@hitit.edu.tr

Research Article

Article History:
Received: 21.03.2024
Accepted: 04.04.2024
Published online: 25.06.2024

Keywords:
Chitosan coated silver nanoparticles
Green synthesis
Antiproliferative activity
Antimicrobial activity
Silver nanoparticles

ABSTRACT

The production of silver nanoparticles (AgNPs) using green synthesis methods promotes the use of environmentally friendly materials and facilitates a more sustainable production process by reducing environmental impact. In addition, combining the metal nanoparticles with biopolymers are getting important to enhance the safety profiles of formulations to determine the biological activities. With this concept, AgNPs were synthesized by green synthesis method from *Betula* spp. tree branches. In our previous study, silver nanoparticles were synthesized and characterized from tree branches, and in this study, similarly synthesized AgNPs were coated with one of the biopolymers. Herein, Chitosan was used as capping and stabilizing agent. Characterization of the biosynthesized silver nanoparticles (AgNPs) and Chitosan coated silver nanoparticles (Ch-AgNPs) were evaluated with various techniques. Through these analyzes, it was elucidated that the phenolic compounds present in *Betula* extract and Chitosan played dual roles as both reducing and capping agents, facilitating the formation of Ch-AgNPs.

Particular size analysis by dynamic light scattering (DLS) and scanning electron microscopy (SEM) indicated that the Ch-AgNPs ranged from 49 to 118 nm in size, with a narrow size distribution. X-Ray Differentiation (XRD) patterns confirmed the high crystallinity of the resulting particles. Fourier transform infrared (FTIR) analysis further supported these findings, revealing the involvement of phenolic compound extracts in both the formation and stabilization of AgNPs. Additionally, FTIR confirmed the surface modification of AgNPs by chitosan. The efficiency of surface modified Ch-AgNPs was compared with uncoated AgNPs for their antimicrobial activity, antiproliferative activity and biocompatibility. Cell culture studies demonstrated that AgNPs were less toxic to L929 cells while maintaining effective cytotoxicity against HT-29 cells. Moreover, surface modification with chitosan enhanced the toxicity of AgNPs against HT-29 cells. Furthermore, the first synthesized and evaluated Ch-AgNPs with this study from *Betula* extract, exhibited potent antimicrobial activity against both Gram-positive and Gram-negative bacteria. Our findings indicate that novel synthesized Ch-AgNPs formula may present a biocompatible and safety approach for further anticancer and antimicrobial studies.

Kitosan Kaplı Gümüş Nanopartiküllerin (Ch-AgNP'ler) Yeşil Sentezi: Sürdürülebilir ve Güvenli Nanomateryal Üretimi için Doğadan Yararlanım

Araştırma Makalesi

ÖZ

Makale Tarihçesi:
Geliş tarihi: 21.03.2024
Kabul tarihi:04.04.2024
Online Yayınlanma: 25.06.2024

Anahtar Kelimeler
Kitosan kaplı gümüş nanopartiküller
Yeşil sentez
Antiproliferatif etkinlik
Antimikrobiyal etki
Gümüş nanopartiküller

Yeşil sentez yöntemleri kullanılarak gümüş nanopartiküllerin (AgNP'ler) üretimi, çevre dostu malzemelerin kullanımını teşvik etmekte ve çevresel etkiyi azaltarak daha sürdürülebilir bir üretim sürecini kolaylaştırmaktadır. Ayrıca metal nanopartiküllerin biyopolimerlerle birleştirilmesi, biyolojik aktivitelerin belirlenmesine yönelik formülasyonların güvenlik profillerinin arttırılması açısından önem kazanmaktadır. Bu konseptle, AgNP'ler *Betula* spp.'den yeşil sentez yöntemiyle sentezlendi. Daha önceki çalışmamızda ağaç dallarından gümüş nanopartikülleri sentezlenip karakterize edilmişti ve bu çalışmada da benzer şekilde sentezlenen AgNP'ler biyopolimerlerden biri ile kaplandı. Burada kapatma ve stabilizasyon ajanı olarak Kitosan kullanıldı. Biyosentezlenen gümüş nanopartiküllerin (AgNP'ler) ve Kitosan kaplı gümüş nanopartiküllerin (Ch-AgNP'ler) karakterizasyonu çeşitli tekniklerle değerlendirildi. Bu analiz sayesinde, *Betula* ekstraktı ve Kitosan'da bulunan fenolik bileşiklerin, Ch-AgNP'lerin oluşumunu kolaylaştırarak hem indirgeyici hem de kapatıcı ajanlar olarak ikili rol oynadığı açıklandı.
Dinamik ışık saçılımı (DLS) ve taramalı elektron mikroskobu (SEM) ile yapılan boyut analizi, Ch-AgNP'lerin boyutlarının 49-118 nm arasında değiştiğini ve dar bir boyut dağılımına sahip olduğunu gösterdi. X-Işını Kırınım (XRD) desenleri, elde edilen parçacıkların yüksek kristalliğini doğruladı. Fourier dönüşümü kızılötesi (FTIR) analizi bu bulguları daha da destekledi ve fenolik bileşik ekstraktlarının AgNP'lerin hem oluşumunda hem de stabilizasyonunda rol oynadığını ortaya çıkardı. Ek olarak FTIR, AgNP'lerin kitosan tarafından yüzey modifikasyonunu doğruladı. Yüzeyi değiştirilmiş Ch-AgNP'lerin etkinliği, antimikrobiyal aktiviteleri, antiproliferatif aktiviteleri ve biyouyumlulukları açısından kaplanmamış AgNP'lerle karşılaştırıldı. Hücre kültürü çalışmaları, AgNP'lerin L929 hücreleri için daha az toksik olduğunu ve HT-29 hücrelerine karşı etkili sitotoksisiteyi koruduğunu gösterdi. Ayrıca, kitosan ile yüzeyi modifiye AgNP'lerin HT-29 hücrelerine karşı toksisitesini artırmıştır. Ayrıca, bu çalışmayla *Betula* ekstraktından sentezlenen ve değerlendirilen ilk Ch-AgNP'ler, hem Gram-pozitif hem de Gram-negatif bakterilere karşı güçlü antimikrobiyal aktivite sergiledi. Bulgularımız, yeni sentezlenen Ch-AgNP formülünün ilerideki antikanser ve antimikrobiyal çalışmalar için biyouyumlu ve güvenli bir yaklaşım sunabileceğini göstermektedir.

To Cite: Kara A., Ozcelik B. Green Synthesis of Chitosan-Coated Silver Nanoparticles (Ch-AgNPs): Harnessing Nature for Sustainable and Safe Nanomaterial Production. Osmaniye Korkut Ata Üniversitesi Fen Bilimleri Enstitüsü Dergisi 2024; 7(3): 1319-1341.

1. Introduction

Nanotechnology has emerged as a transformative field with profound implications for the diagnosis, treatment, and management of various diseases, including cancer and infectious diseases. The ability to manipulate materials at the nanoscale enables the development of innovative therapeutic strategies that leverage unique physical, chemical, and biological properties. Nanotechnology offers promising solutions to address key challenges, including drug resistance, limited efficacy, and off-target effects associated with conventional therapies (Ho et al., 2017; Malik et al., 2023). Silver nanoparticles are significant promising agents in the treatment of cancer and infectious diseases with their activity in disrupting microbial cell membranes and inhibiting the growth of bacteria, viruses and fungi. Since they are low-cost, scalable and biocompatible, especially with green synthesis methods, their use in biomedical applications for drug delivery, diagnosis and treatment makes them ideal carrier system candidates (Mikhailova 2020; Hou et al., 2023; Takáč et al., 2023). Additionally, AgNPs can be engineered for targeted drug delivery, enhancing the efficacy of conventional therapies while minimizing adverse effects on healthy cells. Their diagnostic capabilities enable early disease detection

and monitoring of treatment response, contributing to improved patient outcomes. Furthermore, AgNPs exhibit theranostic potential, integrating therapy and diagnostics into a single platform (Burdușel et al. 2018). Advances in nanoparticle synthesis have led to formulations with improved biocompatibility and biodegradability, addressing concerns about toxicity and long-term accumulation. Continued researchs and developments in this field are crucial for realizing the full therapeutic potential of AgNPs and translating them into clinical practice. Among the methods of synthesizing AgNPs, green synthesis is considered particularly important due to its sustainability, environmentally friendly, and potential for biomedical applications. Unlike conventional chemical synthesis methods, which often involve the use of toxic chemicals and solvents, green synthesis utilizes natural, non-toxic, and renewable resources such as plant extracts, microbial agents, or biocompatible polymers. This approach not only reduces the environmental footprint associated with nanoparticle production but also eliminates the generation of hazardous by-products. Furthermore, green synthesis methods are typically cost-effective, energy-efficient, and scalable, making them suitable for large-scale production. The use of biologically synthesized in medical fields has indeed shown promise, particularly in areas such as wound healing, antibacterial coatings, and drug delivery systems (Rautela et al., 2019; Asif et al., 2022; Giri et al., 2022). However, concerns about their potential cytotoxic effects have tempered widespread adoption. AgNPs can exert cytotoxic effects on various cell types, including human cells, through mechanisms such as oxidative stress, DNA damage, and disruption of cellular processes. While these effects can be beneficial in targeting pathogens or cancer cells, they also raise concerns about potential harm to healthy cells (Akter et al., 2017; Liao et al., 2019). Surface modifications, such as coating AgNPs with biocompatible materials or functionalizing them with targeting ligands, can enhance their biocompatibility and specificity. Coating enhances the stability of AgNPs, preventing aggregation and preserving their unique properties, which is vital for maintaining their efficacy over time. Moreover, coating allows for controlled release of encapsulated substances, enabling precise delivery of therapeutic agents for targeted treatments. Additionally, functionalization of the coating enables customization, facilitating attachment of targeting ligands or other molecules for specific applications such as targeted drug delivery or diagnostic imaging. It is essential to coat with biocompatible materials to ensure the safety of AgNPs in biological environments, mitigating potential cytotoxicity and facilitating their interaction with biological systems. Biocompatible shell acts as a protective barrier, minimizing direct contact between the silver core and living tissues or cells (Jeon and Baek, 2010; Abedin et al., 2018; Zentel, 2020; Komsthöft et al., 2022). The coating of AgNPs can indeed significantly alter their properties, and these changes are influenced by both the type of coating material and the thickness of the coating layer. Chitosan, a biopolymer derived from chitin, has attracted significant attention in biomedical applications owing to its biocompatibility, biodegradability, and versatile chemical properties (Jimenez-Gomez and Cecilia, 2020; Desai et al., 2023). The conjugation of chitosan with AgNPs not only enhances their stability and dispersibility but also augments their therapeutic potential, making them promising candidates for combating microbial infections and cancer. Chitosan's mucoadhesive properties enable

targeted drug delivery to mucosal tissues, and its pH responsiveness allows for controlled release of therapeutics. Additionally, its film-forming ability makes it particularly well-suited for applications requiring thin protective coatings. Moreover, chitosan's ease of modification facilitates the incorporation of additional functionalities into AgNP-chitosan composites (Di Martino et al., 2017; Maslamani et al., 2022; Wang et al., 2022; Farhadi et al., 2022). In our previous report, silver nanoparticles were synthesized from *Betula* tree branched extracts by green synthesized method and characterized for their nanoparticular features (Özcelik and Kara, 2023). In this study, it was aimed to synthesize Ch-silver nanoparticles using a green approach, employing *Betula* extract as the reducing and capping agent. The fabricated nanoparticles were characterized comprehensively using various analytical techniques to elucidate their physicochemical properties. Furthermore, the anticancer efficacy and antimicrobial activity of the synthesized nanoparticles were evaluated *in vitro*, aiming to elucidate their potential as dual-function therapeutic agents. This research represents a step towards the development of sustainable and effective nanotherapeutics for combating microbial infections and cancer, addressing critical challenges in healthcare and biomedicine.

2. Materials and Methods

2.1. Materials

Silver nitrate ($AgNO_3$), low molecular weight chitosan (deacetylation degree 75–85%), acetic acid glacial (CH_3COOH, 99%), ethanol (C_2H_5OH, 99%) Muller Hilton Broth, 3-(4,5-dimethylthiazol-2-yl)-2,5-diphenyltetrazolium bromide (MTT), and dimethyl sulfoxide (DMSO) were supplied from Sigma-Aldrich (St Louis, MO, USA). Dulbecco's Modified Eagle's Medium (DMEM) high glucose, and pyruvate were purchased from Gibco (Waltham, MA, USA). *Escherichia coli* (ATCC 25922), *Pseudomonas aeruginosa* (ATCC 27853), gram-positive bacteria, *Staphylococcus aureus* (ATCC 25923), *Enterococcus faecalis* (ATCC 29212) and a yeast, *Candida albicans* (ATCC 10231) strains were acquired for antimicrobial research. Human Caucasian colon adenocarcinoma cell line HT29 (ATCC HTB-38) and L929 mouse fibroblast cell line was purchased from ATCC Cell Bank (USA) to determine antiproliferative activity and biocompatibility of AgNPs and Chitosan coated-AgNPs (Ch-AgNPs) formulations. All chemicals were of analytical purity.

2.2. Methods

2.2.1. Preparation of plant extracts

The extraction of plant branches was performed according to our previous study as indicated below (Ozcelik and Kara, 2023). Brances of *Betula* plant which were sourced from Van province, Türkiye as reported before, underwent purification by washing twice with distilled water and were then air-dried at room temperature in the shade. Following drying, the branches were finely ground using an electric grinder and weighed. Subsequently, 25 g of the dried ground samples were blended with 10 times the liquid volume of purified water.

The extraction procedure was carried out using a Soxhlet device at 80°C for a duration of 8 h. Following extraction, the resulting solution underwent filtration using Whatman No. 1 filter paper. It was then carefully stored at a temperature of 4°C to facilitate future investigation and analysis (Hradılova et al., 2018). All procedures were conducted in duplicate.

2.2.2. Green Synthesis of silver nanoparticles (AgNPs)

Silver nanoparticles were prepared from plant branches according to our optimized conditions as previously mentioned in literature (Deveraj et al., 2013; Ozcelik and Kara, 2023). Herein, silver nitrate ($AgNO_3$) was used as an initiator to get AgNPs. Based on this, $AgNO_3$ solution was prepared in 3mM concentration and incubated with plant branches extracts as a bio reductor in the ratio 1:10 for 4 h at 80 ˚C.

The validation of the synthesis of silver nanoparticles was confirmed by observing noticeable changes in the color of the solution. Subsequently, to purify the nanoparticles, centrifugation was conducted at a speed of 13500 rotations per minute for a duration of 20 minutes (Sigma 3-30KS, Germany) and replicated twice to ensure removal of any residual silver ions. After centrifugation, the supernatant was delicately decanted, and the ensuing pellet was left to air dry overnight in an incubator, resulting in the formation of a powdered substance. This entire process was conducted twice to validate the experimental results.

2.2.3. Preparation of chitosan coated AgNPs

AgNPs previously synthesized by reduction with *Betula* extract served as the initial material for the coating process. Low molecular weight chitosan (≥75% degree of deacetylation) was used to coat AgNPs. The coating process for the AgNPs with chitosan was adapted from a previously documented protocol with minor adjustments (Raza et al., 2021). Briefly, 15 mg/ml chitosan solution in % 1 glacial acetic acid was prepared and then filtered through 0.22 μm sized syringe filtre to remove insoluble particles. 5 mL of AgNPs solution was added dropwise to the freshly prepared chitosan solution under constant stirring (1000 rpm) and incubated at the dark for 4 h. The resulting mixture was heated by microwave at 650 W for 90 seconds with 30-second intervals to facilitate the interaction between chitosan and AgNPs. After microwave treatment, the suspension containing the fabricated nanocomposite system was then centrifuged at 14.000 rpm for 20 min at 4 °C. The obtained pellets were washed three times with deionized water to eliminate any unbound residues. The Ch-AgNPs were lyophilized and kept at 4 °C for subsequent characterization. The influence of different volume ratio of chitosan solution: AgNPs suspension on the physicochemical properties of the resulting nanoformulation was evaluated.

2.2.4. Characterization of AgNPs and Ch-AgNPs

Uncoated and chitosan-coated AgNPs were characterized by various methods. UV-Vis spectroscopy was employed to characterize the silver nanoparticles synthesized through green methods with their spectra measured across the 200-800 nm range via an UV-visible spectrophotometer (Rayto, RT, 2100C, China). The particular features (e.g. size, zeta potential and polydispersity index) of silver nanoparticles and chitosan coated forms were evaluated via dynamic light scattering method. Each data collection was conducted at 25°C, with fresh sample preparations made for every analysis. The experimental procedure was replicated three times to ensure the robustness of the results. The morphological characterizations of AgNPs and Ch-AgNPs were evaluated by Scanning Electron Microscopy (SEM) (FEI / Quanta 450 FEG, Japan). Subsequently, Fourier Transform Infrared Spectroscopy (FTIR) (Thermo Scientific / Nicolet IS50, China) was used to determine the nature of functional groups both before and after the application of chitosan coating. The measurements were conducted within the spectral range from 400 to 4000 cm^{-1} was examined using the KBr pellet method with a resolution of 4 cm^{-1}. Also, silver nanoparticles and chitosan-coated silver nanoparticles were characterized by X-Ray Diffraction (XRD) (Rigaku DMAX 2200) method to determine the crystal structural of both formulations to verify the coating has occurred.

2.2.5. Determining antiproliferative activity of NPs and Ch-AgNPs

Uncoated and Ch-AgNPs were evaluated for their antiproliferative activity on HT29 colorectal cancer cell line by (3-(4,5-dimethylthiazol-2-yl)-2,5-diphenyltetrazolium bromide) (MTT) assay (Saeidi et al., 2020). Cells were seeded at a density of $1x10^4$ cells/well in 96-well plates and were cultured in DMEM medium supplemented with 10% FBS and 1% pen-strept solution at 37°C in 5% CO_2. The medium was refreshed upon cells reaching 70-80% confluency within 48 hours. The cells were sub-cultivated with trypsin-EDTA solution (0.05%) after confluency. Then cells were subjected to overnight serum starvation before exposure to formulations. Subsequently, the cell culture medium was substituted with the medium was enriched with serum (100 µL), and treated with varying concentrations of AgNPs and Ch-AgNPs (20–100 µg/mL) dispersed in serum-free medium for 24 and 48 hours. After the designated incubation duration, 25 µL MTT (5 mg/mL) was added to each well and incubated at 37°C with 5% CO_2 for 4 hours. Subsequently, the culture medium was aspirated, and 200 µL of DMSO was added to dissolve the formazan crystals. Absorbance was measured at 570 nm using a plate reader, and results were normalized to non-treated cells as following the viability (%) was determined by calculating the absorbance percentage relative to that of the untreated cells. The absorbance of non-treated cells was accepted as 100 %, the absorbance of treated cells was calculated according to the non-treated cell values. The experimental prosedure was performed in triplicate to ensure data reliability. The experimental prosedure was conducted in triplicate.

2.2.6. Determining biocompatibility of AgNPs and Ch-AgNPs

To determine the biocompatibility of AgNPs and Chitosan-coated AgNPs formulations, L929 cells was used. As indicated in antiproliferative activity studies, cells were added to each well of 96-well plats for growing and treated with varying concentrations of AgNPs and Ch-AgNPs (20–100 µg/mL) dispersed in serum-free medium for 24 and 48 h. Following incubation, 25 µL of MTT solution (5 mg/mL) was introduced to each well and allowed to incubate for 4 h. Afterward, 200 µL of DMSO was added to dissolve the resulting formazan crystals, and absorbance measurements were conducted using a microplate spectrophotometer set at 570 nm. The experimental prosedure was conducted in triplicate.

2.2.7. Antimicrobial activity of AgNPs and Ch- AgNPs

The antimicrobial activity of silver nanoparticles (AgNPs) and chitosan-coated silver nanoparticles (Ch-AgNPs) were assessed using a panel of microorganisms including gram-negative bacteria *Escherichia coli* (ATCC 25922) and *Pseudomonas aeruginosa* (ATCC 27853), gram-positive bacteria *Staphylococcus aureus* (ATCC 25923) and *Enterococcus faecalis* (ATCC 29212), as well as the yeast *Candida albicans* (ATCC 10231). The Kirby–Bauer Disk method was employed for this evaluation, following the protocol previously described (Ozcelik and Kara, 2023). In brief, bacterial and fungal suspensions were prepared at a concentration of 10^6 colony-forming units (cfu) per spot and inoculated onto Mueller–Hinton Agar (MHA) and Sabouraud Dextrose Agar, respectively. 147 µL and 196 µL of silver nanoparticle stock solution were added to impregnate 15 µg and 20 µg silver nanoparticles to the discs, respectively. Positive controls, including gentamicin for bacteria and fluconazole for fungi, were used, while negative controls comprise disks applied with sterile medium. The plates were incubated at 37 °C for 48 h. Following the incubation period, the dimensions of the zones of inhibition measured (as mm) to assess the antibacterial and antifungal activities of AgNPs and Ch-AgNPs against the tested microorganisms. Three replicates of the experiments were performed to ensure the reliability of the results.

2.2.8. Minimal inhibitory concentration (MIC) of AgNPs and Ch-AgNPs to test microorganisms

The microdilution technique serves as a broadly recognized and sensitive approach to systematically assess the antimicrobial properties and determine the Minimum Inhibitory Concentration (MIC) values. As described previously, the minimum inhibitory concentration values of AgNPs and Ch-AgNPs to the selected test microorganisms were determined through the broth microdilution technique (Ozcelik and Kara, 2023). The test microorganisms were prepared at a concentration of 1×10^4 colony-forming units per milliliter (CFU/mL) and incubated with AgNPs and Ch-AgNPs, which were diluted in Mueller-Hinton Broth (MHB) to achieve varying amount spanning from 0.046 to 60 µg/mL. Non-treated neither AgNPs nor Ch-AgNPs were included as controls. The micro-well plates containing the microbial suspensions and nanoparticles were then incubated at 37 ± 1°C for 24 h. Following incubation, the MIC was determined as the lowest concentration of AgNPs or Ch-AgNPs at which no visible microbial

growth was observed. This concentration was identified by visual inspection, with the first well showing no visible growth considered as the MIC. The MIC values were expressed in micrograms per milliliter (μg/mL). All tests were performed in triplicate to ensure accuracy and reproducibility of the results.

2.2.9. Statistical analysis

All data are presented as mean ± standard deviation (SD) in triplicates. The statistical significance was determined using SPSS software. All results of formulations were statistically evaluated using two-way ANOVA (*p<0,05) to identifiy the significance.

3. Results and Discussion

3.1. Characterization of AgNPs and Ch-AgNPs

Green synthesis of silver nanoparticles (AgNPs) was carried out with interaction a precursor $AgNO_3$ with *Betula* branch extract which is reducing agents with it is biological active content (Saxena et al., 2013). This reaction is based on the formation of silver nanoparticles by reducing silver ions (Ag^+) into neutral silver (Ag^0) aggregates in the presence of a reducing agent. Plants as a reducing agent contains some biomolecules as flavonoid, enzyme, alkaloids, terpenes, phenols, polysaccharides, tannis (Wulandari et al, 2022). So that, this biological synthesis route offers advantages, thus enabling a reduction in the use of harmful toxic substances. Initially, confirmation of silver nanoparticle formation was achieved through the observation of a distinct color change in the solution, typically indicative of a chemical reaction taking place. In our previous study, we have determined the optimum AgNPs synthesis parameters in terms of $AgNO_3$ concentrations and ratio to *Betula* extract, reaction time and temperature (Ozcelik and Kara, 2023). Therefore, in this study AgNPs were synthesized by mixing 3 mM $AgNO_3$ solution with *Betula* branches extract in a 1:10 ratio at 80 ˚C. As shown in Figure 1. the color of $AgNO_3$ solution was changed from yellow to brownish dark yellow within 4h. This color changes indicated the reduction of Ag^+ to neutral Ag^0 which AgNPs were synthesized (Azizi et al., 2013; Jalab et al., 2021).

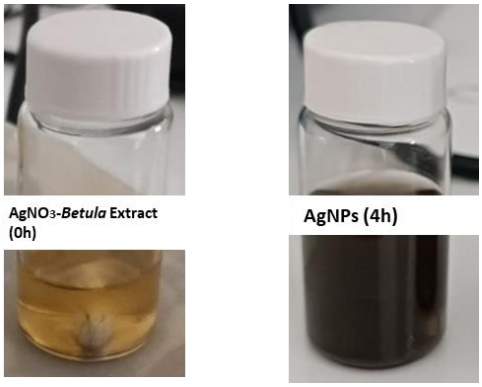

Figure 1. The color change of silver nitrate solution after incubating the *Betula* extract within 4 h of incubation at 80 ˚C.

In this study, AgNPs were synthesized through a reduction process facilitated by the properties of the plant extract. Subsequently, a coating process was employed to coat the AgNPs with low molecular weight chitosan, forming a nanocomposite material. The resulting AgNPs and Ch-AgNPs were further confirmed using UV-Vis spectrophotometer, FTIR, XRD and characterized in terms of physicochemical parameters by DLS and SEM. Additionally, the study evaluated the influence of the chitosan solution to AgNPs solution ratio on the properties of the Ch-AgNPs. By varying the ratio of chitosan solution to AgNPs solution, it was examined how this parameter affected the characteristics and performance of the resulting Ch-AgNPs. This investigation aimed to elucidate the optimal ratio that would yield desired properties such as particle size, stability, and zeta potential, providing valuable insights into the formulation and optimization of Ch-AgNP nanocomposites for potential medical applications. Table 1 showed the physicochemical properties of both AgNPs and Ch-AgNPs. The results provide significant insight that upon chitosan coating, there was an increase in the mean particle size of the AgNPs, suggesting that the chitosan layer added thickness to the nanoparticles. Additionally, the polydispersity index (PDI) decreased in the Ch-AgNPs compared to the uncoated counterparts. This decrease in PDI indicates a reduction in the heterogeneity of particle size distribution, signifying enhanced uniformity and stability conferred by the chitosan coating. Indeed, the study revealed distinct outcomes based on the ratio of chitosan solution to AgNPs solution. When equal volumes of chitosan solution and AgNPs solution were utilized, a larger PDI was observed. This suggests a wider range of particle sizes and increased heterogeneity in the resulting nanocomposite. Conversely, when the chitosan solution volume was three times that of the AgNPs solution, larger particles were formed, indicating possible aggregation or clustering of nanoparticles. However, the optimal ratio was found when the chitosan solution volume was twice that of the AgNPs solution, resulting in desirable characteristics. These findings underscore the importance of the chitosan to AgNPs solution ratio in controlling the properties of the resulting nanocomposite, offering valuable insights for the design and optimization of Ch-AgNPs for medical applications. Indeed, the chitosan coating resulted in a positive zeta potential of the nanoparticles, which also further validated the successful coating of the chitosan on the surface of the AgNPs. This positive zeta potential is a characteristic feature of chitosan, which is a positively charged polysaccharide due to the presence of amino groups in its structure. This positive charge can enhance the stability of the nanoparticles in suspension by electrostatic repulsion between particles, preventing agglomeration or sedimentation. Additionally, the positively charged surface of Ch-AgNPs may facilitate interactions with negatively charged molecules or surfaces, enabling various applications such as drug delivery and antimicrobial activity. The results were consistent with those reported in prior studies by Raza et al., 2021 and Constantin et al., 2022. Ch-AgNPs prepared according to AgNPs:chitosan solution ratio (1:2) were selected as an optimum formulation for further studies.

Table 1. Physicochemical properties of AgNPs and Ch-coated AgNPs. The data were presented as the mean ± standard error of the mean (SEM) values derived from three independent batches.

Formulations	AgNPs:CS solution ratio (v/v)	Mean particle size (nm)	Polydispersity index	Zeta potential (mV)
AgNPs	-	106.4 ± 3.1	0.26 ± 0.02	-21.5 ± 4.8
Ch-AgNPs	1:1	113.5 ± 2.7	0.28 ± 0.01	+26.2 ± 3.5
Ch-AgNPs	1:2	118.2 ± 1.6	0.21 ± 0.01	+27.3 ± 4.7
Ch-AgNPs	1:3	145.4 ± 1.8	0.24 ± 0.03	+29.5 ± 6.3

The synthesis of AgNPs and Ch-AgNPs was confirmed through UV–Vis spectroscopy method by comparing the particular absorbance peaks of formulations in the range of 200-800 nm. As indicated in our previous study, despite the absence of discernible absorbance peaks in the UV-Vis spectrum of the *Betula* plant branches extract, the AgNPs exhibited a maximum absorbance peak at 425 nm (Ozcelik and Kara, 2013). In current study, UV-Vis spectrum of Ch-AgNPs was evaluated to determine the surface plasmon resonance (SPR) band of AgNPs. As shown in Figure 2 Ch-AgNPs showed mainly single sharp peak at also 425 nm demonstrated that the AgNPs were synthesized successfully as reported in literatures (Cinteza et al., 2018; Huq et al., 2022; Farhadi et al., 2022). This observed characteristic higher and sharp peak for Ch-AgNPs indicating that the biopolymer chitosan stabilized the AgNPs with a narrow distribution efficiently and this result also supported by our particle size and polydispersity index analysis. It is reported also in previous studies that absorption peaks of silver nanoparticles and coated forms are associated with morphology, size, shape and distribution nanoparticles (Imran et al., 2020; Shinde et al., 2021).

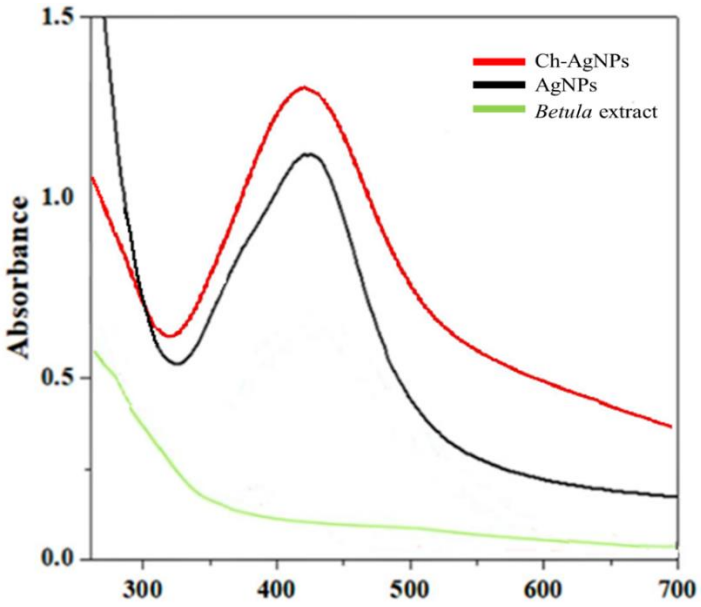

Figure 2. UV–Vis absorption spectra of *Betula* plan extract, AgNPs and Ch-AgNPs

The reduction of silver ions to AgNP is attributed to the presence of functional groups especially (-OH) within the phytocomponents as Tannis of *Betula* plant extracts. Therefore, Fourier transform infrared Spectroscopy (FT-IR) analysis of AgNPs and Ch-AgNPs was conducted to verify the molecular interaction between the coated and uncoated AgNPs by determining the status of the functional groups. In our previous study, we revealed the formation of AgNPs comparing with FT-IR spectral peaks of plant extract (Ozcelik and Kara, 2023). As indicated previously, observed main AgNPs absorption peaks revealed the formation of AgNPs which is consistent with literature (Mallikarjuna et al., 2011). Also, the absence of peaks corresponding to functional groups in *Betula* extract confirmed this result. In current study, FT-IR spectrums of AgNPs and Ch-AgNPs were evaluated to determine whether the capping of chitosan to the surface of AgNPs has been occurred successfully. As seen in Figure 3 the main FT-IR spectral peaks were observed at 3489, 2902, 1654 and 1004 cm^{-1} for AgNPs (blue line) which showed similar peak models with Ch-AgNPs as 3301, 1618, 1504, 1364 and 1003 cm^{-1} for Ch-AgNPs (black line). The FT-IR analysis revealed the presence of specific several functional amino groups peaks in Ch-AgNPs which introduced as capping agents as indicated in literatures (Shinde et al., 2021; Kalaivani et al., 2018; Rathod et al., 2016). As seen in Figure 3 the characteristic peak at 3489 cm^{-1} in AgNPs showed low density when compared with Ch-AgNPs suggesting stretching vibrations of O-H or N-H groups. The similar peak for Ch-AgNPs at 3301 cm^{-1} indicating an increased presence of O-H groups, while the involvement of N-H groups in binding to the silver metal is implied. Also, the peak of amide II band at 1504 cm^{-1} presents that all the O-H and N-H functional groups both demonstrate a significant affinity for silver ions.

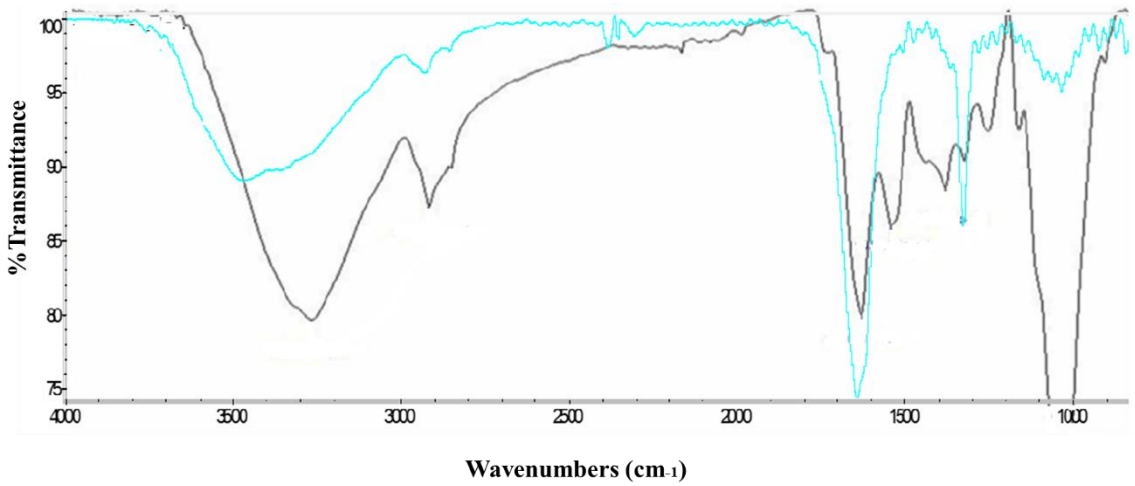

Figure 3. FTIR spectrum of AgNPs (Blue line) and Ch-AgNPs (Black line)

Nate et al. reported also similar results to ours that the existence of these functional groups on the surface of the synthesized silver nanoparticles, coupled with the disappearance of the NH_2 double peak, suggests the successful encapsulation of the nanoparticles by the polymer (Nate et al, 2018). The FT-IR spectrum findings demonstrated that the reduction was occurred, chitosan capped the surface of AgNPs and these identified amino groups play a crucial role in interacting with the metal surface, serving as sites for the stabilization of AgNPs (Shinde et al., 2021; Kalaivani et al., 2018; Rathod et al., 2016).

The crystal structure of AgNPs and Ch-AgNPs was characterized by X-Ray Diffraction (XRD) analysis. According to XRD patterns, AgNPs showed four main characteristic peaks at 38,22°, 44,38°, 64° and 77,8° at 10 to 100 2Θ degree which is point out (111), (200), (220) and (311) respectively. These values showed similarity with literature that silver nanoparticles have cubic spherical structure with silver-centered crystalline which was confirmed by TEM images (Govindan et al., 2012; Panja et al., 2016). As seen in Figure 4 AgNPs and Ch-AgNPs showed very similar XRD patterns that is far from impurities as reported in literatures. Our results showed similarity with previous reports that high similarity XRD patterns of AgNPs and Ch-AgNPs suggest that the silver nanoparticles remain stable by unchanging the crystal structure following the coating with chitosan (Ateş et al., 2021; Jyoti et al., 2016).

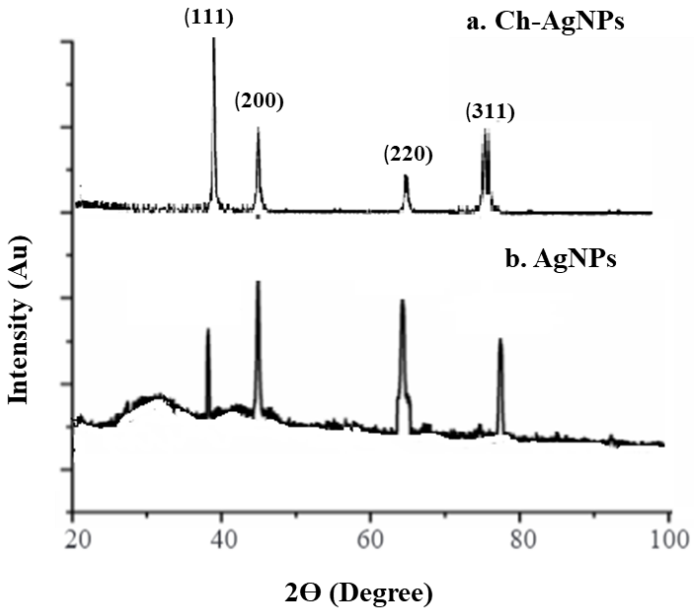

Figure 4. XRD Spectrum of a. Ch-AgNPs and b. AgNPs

The morphological characterization of Ch-AgNPs was performed using SEM. SEM analysis of the Ch-AgNPs provided complementary insights not only into their morphology but also into size distribution. SEM analysis confirmed that Ch-AgNPs have sizes between 49.75±1.7 and 70.0±5.6 nm in dried state. It was observed that the mean particle size obtained from SEM analysis was smaller than the results obtained from DLS. This discrepancy between the two techniques is frequently observed and can be attributed to inherent differences in measurement principles and methodologies. SEM analysis typically measures the size of the dry particles on a solid substrate, which may lead to particle shrinkage and underestimation of the actual particle size compared to DLS which measures the hydrodynamic size of particles in solution based on their Brownian motion (Souza et al., 2016). The SEM analysis also revealed that the Ch-AgNPs exhibited a spherical shape (Figure 5). This observation indicates that the chitosan coating did not significantly alter the overall morphology of the nanoparticles, which retained their characteristic spherical structure. The spherical shape of the nanoparticles is consistent with typical AgNP morphology and is often desired for various applications due to its uniformity and high surface-to-volume ratio. The preservation of spherical morphology after chitosan coating suggests that the chitosan layer formed a conformal coating around the nanoparticles without causing significant distortion or aggregation. This is important as it ensures the structural integrity and stability of the Ch-AgNPs, which are crucial for their performance in applications such as drug delivery.

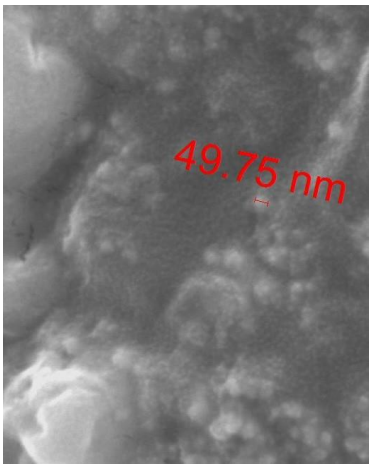

Figure 5. Scanning electron microphotographs of Ch-AgNPs

3.2. Antiproliferative activity of AgNPs and Ch-AgNPs against HT-29 CRC cell line

Polymer-based surface modification is a widely employed strategy aimed at enhancing various aspects of drug delivery systems. By modifying the surface of drug carriers, such as nanoparticles or microparticles, with polymers, several beneficial properties can be achieved, including improved penetration capability, controlled drug release, drug targeting to specific sites, and increased drug payload capacity. For this reason, following the characterization analyses, antiproliferative activity of nanoparticles against HT-29 CRC cells were evaluated. To conduct this assessment, HT-29 CRC cells were treated with both AgNPs and Ch-AgNPs at various concentrations for 24 h and 48 h. Cell viability was then measured using MTT assay which assess metabolic activity and cell viability based on the conversion of colorimetric substrates by viable cells and the half-maximal inhibitory concentrations (IC_{50}) were determined for nanoparticles. The Figure 6A and B demonstrated that increasing concentrations of both AgNPs and Ch-AgNPs resulted in progressively lower cell viability in HT-29 CRC cells. The results also indicated the cell viability of HT-29 cells following 24 and 48 h of incubation both with AgNPs and Ch-AgNPs. It was evident from the results that the toxicity of the nanoformulations increased over time. The half-maximal inhibitory concentration of AgNPs and Ch-AgNPs was determined to be 65.77 µg/mL and 42.3 µg/mL, respectively, following 48 h of treatment. Coating AgNPs with chitosan increases their interaction with negatively charged cell membranes due to the positive charge of chitosan, resulting in increased cellular uptake (Alomrani et al., 2019). Therefore, Ch-AgNPs showed a higher cytotoxic effect on the HT-29 cell line than AgNPs. Our findings are consistent with a prior investigation examining the *in vitro* cytotoxic effects of Ch-AgNPs against MCF-7 human breast cancer cells. The results showing a 64% inhibition of cell proliferation at a concentration of 100 µg/mL highlight the substantial cytotoxic effect of Ch-AgNPs against MCF-7 cells (Parthasarathy et al., 2020). In another study, nanostructured lipid carriers (NLCs) coated with chitosan were assessed for their impact on cell viability. The results showed that both coated NLCs and uncoated NLCs led to a significant decrease in cell viability. However, the reduction in cell viability was more pronounced for

coated NLCs, with a 70% decrease observed, compared to a 50% decrease for non-coated NLCs (Almeida et al., 2022). As seen in Figure 6A the results did not show significant differences which obtained for AgNPs even both time point. But Chitosan-Silver nanoparticles at maximum concentration showed significant differences between 24h and 48 h (*p<0,05).

A)

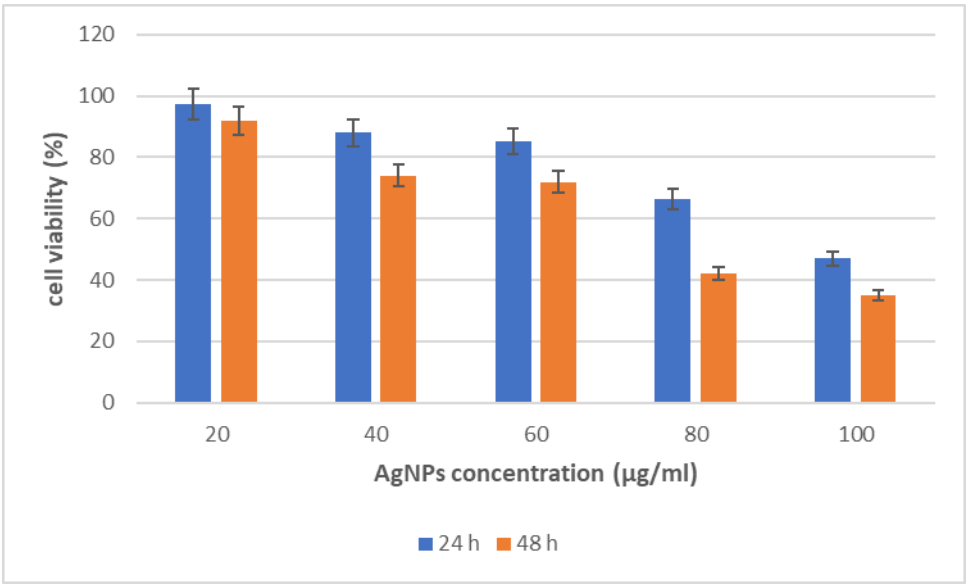

B)

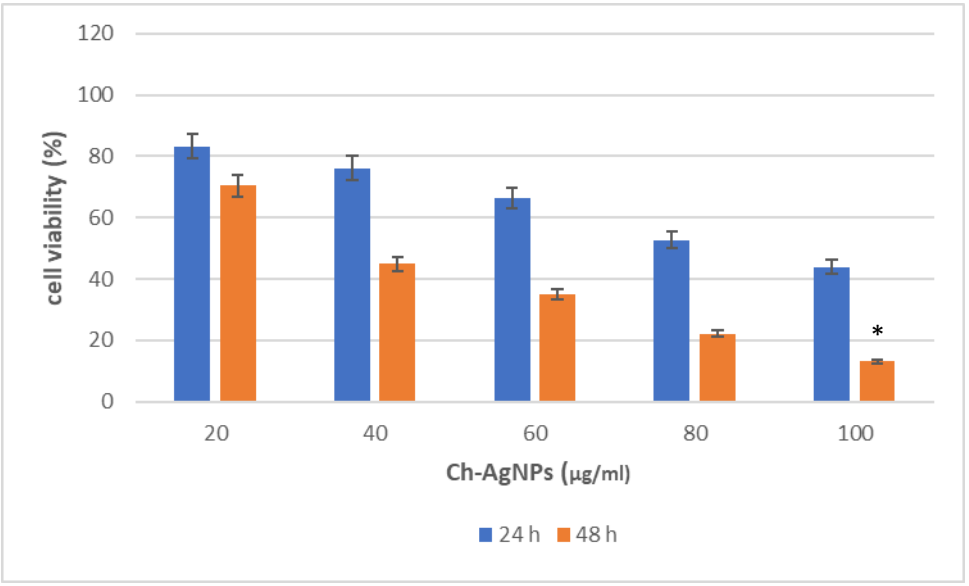

Figure 6. Analysis of the percentage of cell viability in HT-29 cells post-treatment with varying concentrations of both **A)** AgNPs and **B)** Ch-AgNPs.

3.3. Biocompatibility of AgNPs and Ch-AgNPs

The analysis of cell viability in L929 cells following 24 and 48 h of incubation with AgNPs and Ch-AgNPs indicated that the toxicity of the nanoformulations varied with the concentration administered. (Figure 7 A and B). The observed very low cytotoxic effects of both AgNPs and Ch-AgNPs on the L929 cell line, regardless of concentration, suggest that these nanoparticles are biocompatible and do not exhibit dose-dependent cytotoxicity, indicating their potential suitability for biomedical applications. Specifically, the IC_{50} values of AgNPs and Ch-AgNPs were calculated to be be 237.81 µg/mL and 283.95 µg/mL, respectively, after 48 h of treatment. Our results showed that Ch-AgNPs are biocompatible for healthy cells but cytotoxic for cancer cells. The cancer cells typically exhibit a more acidic microenvironment compared to normal cells. This acidic environment facilitates the release of silver ions from nanoparticles, leading to a higher rate of cell death in cancer cells compared to normal cells. Our findings aligned with previous research that demonstrated the the preferential toxicity of biologically synthesized AgNPs against breast cancer cells while exhibiting no adverse effects on mouse fibroblast cells (Khorrami et al., 2018). Our findings were also consistent with a study that indicated the minimal cytotoxicity of both AgNPs and Ch-AgNPs towards L929 cells. The survival rate of L929 cells co-incubated with varying concentrations of AgNPs and Ch-AgNPs exceeded 80% after 24 h (Liu et al., 2022). These findings suggest that AgNPs and Ch-AgNPs are biocompatible and well-tolerated by L929 cells under the conditions tested. As seen in Figure 7A and 7B the results did not show significant differences which obtained for AgNPs and Chitosan-silver nanoparticles even both time point.

A)

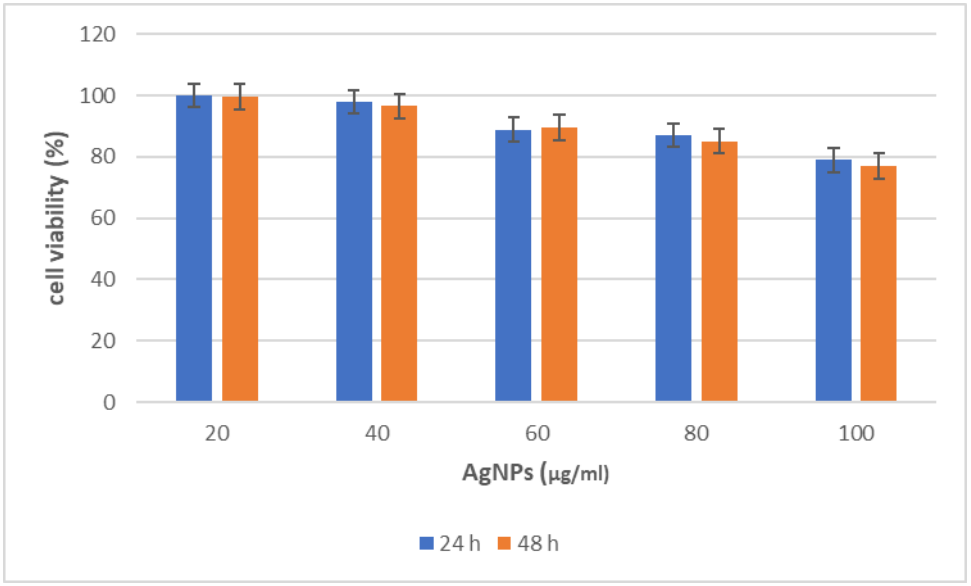

B)

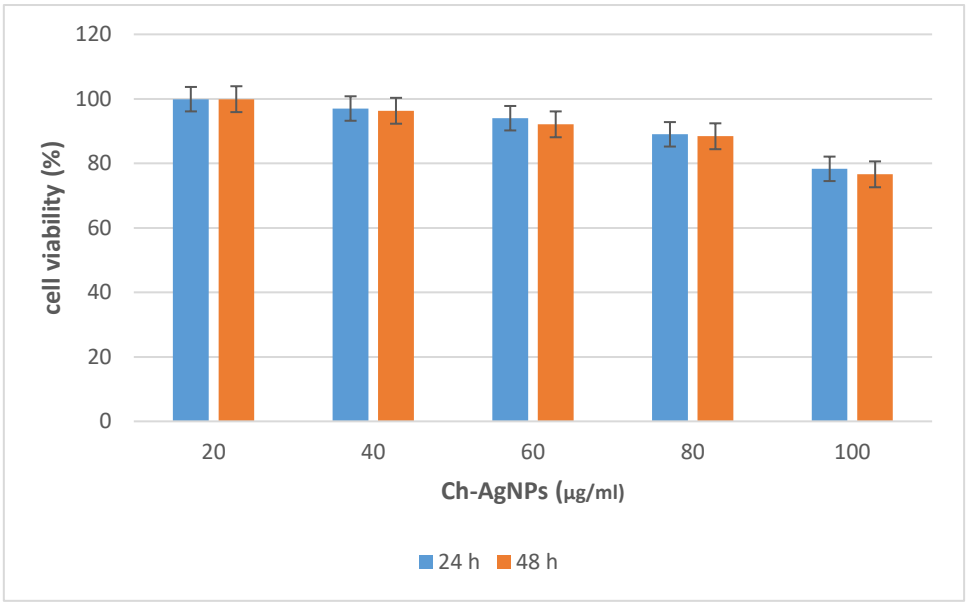

Figure 7. Analysis of the percentage of cell viability in L929 cells post-treatment with varying concentrations of both **A)** AgNPs and **B)** Ch-AgNPs.

3.4. Antibacterial and antifungal activity of AgNPs and Ch-AgNPs

The antimicrobial activity of AgNPs and Ch-AgNPs was assessed against a range of microorganisms, including *Escherichia coli, Pseudomonas aeruginosa, Staphylococcus aureus, Enterococcus faecalis* and *Candida albicans*. The assessment of antimicrobial activity revealed that Ch-AgNPs exhibited substantial zones of inhibition against all tested organisms (Table 2). Remarkably, the zone diameter of inhibition observed for Ch-AgNPs was significantly larger compared to that of bare AgNPs ($p<0.05$). 20 µg/mL AgNPs showed inhibition zones of 13 mm in *Staphylococcus aureus* whereas 20 µg/mL Ch-AgNPs showed inhibition zones of 21 mm in the same test microorganisms. This outcome suggests that the chitosan coating enhances the antimicrobial efficacy of the silver nanoparticles against the tested microorganisms. As seen in Table 2, the mean zone diameters of formulations were evaluated statistically. According to average zone of inhibition, 20 µg/disc Ch-AgNPs showed significant antimicrobial activity against all test microorganisms ($p<0.05$) compared to gentamicine which is compatible with the literature. Chitosan is known for its antimicrobial properties, disrupting the cell membrane integrity of microorganisms. The positively charged chitosan polymer interacts with negatively charged microbial cell membranes, facilitating the adhesion of Ch-AgNPs to microbial surfaces. Additionally, chitosan coating improves the stability and dispersion of AgNPs, ensuring better interaction with microbial cells and enhancing antimicrobial efficacy. Moreover, chitosan may promote the controlled release of silver ions from AgNPs, which possess potent antimicrobial properties. The combined action of chitosan and silver nanoparticles results in synergistic antimicrobial effects, further enhancing overall efficacy against a wide range of microorganisms. Furthermore, Ch-AgNPs can be selectively targeted to sites of infection or microbial colonization, thanks to the targeted delivery

facilitated by chitosan's positive charge (Teixeira-Santos et al., 2021; Yan et al., 2021; Huq et al., 2022). The larger zone diameter of inhibition observed for Ch-AgNPs highlights the potential of this nanocomposite for various antimicrobial applications, including wound dressings and medical devices. This finding underscores the importance of surface modification techniques, such as chitosan coating, in enhancing the antimicrobial performance of nanomaterials, contributing to the development of effective strategies for combating microbial infections. Our findings verified those of a study where the inhibitory effect of Ch-AgNPs was assessed against *Enterococcus faecalis* and *Pseudomonas aeruginosa*. It's notable that the findings contrast with the results from a similar study where no antifungal effect of Ch-AgNPs was observed against *Aspergillus* species (Raza et al., 2021).

Table 2. The mean zone diameters of AgNPs and Ch-AgNPs as measured by disk diffusion method

Test microorganisms	**Average zones of inhibition (mm)**					
	AgNPs (µg/disk)		**Ch-AgNPs (µg/disk)**		**Gentamicin (µg/disk)**	**Fluconazole (µg/disk)**
	15	**20**	**15**	**20**	**10**	**10**
Escherichia coli	14	17	16	21	18	-
Pseudomonas aeruginosa	19	20	23	25	13	-
Staphylococcus aureus	10	13	13	21	19	-
Enterococcus faecalis	19	20	25	25	19	-
Candida albicans	19	21	22	28	-	14

3.5. Minimal inhibitory concentration (MIC) of AgNPs and Ch-AgNPs against test microorganisms

The MIC of both AgNPs and Ch-AgNPs was conducted using the microdilution method in which serial dilutions of the nanoformulations were meticulously prepared to modulate their concentrations across a spectrum ranging from 0.046 to 60 µg/mL. This range determined according to the literature allows for a comprehensive assessment of the antimicrobial activity of the nanoparticles across various concentrations. As seen in Table 3, the Ch-AgNPs demonstrated significantly smaller MIC values compared to bare AgNPs ($p<0.05$). The observation that MIC values for *Escherichia coli, Pseudomonas aeruginosa, Staphylococcus aureus and Enterococcus faecalis* were halved for Ch-AgNPs compared to those of AgNPs. The finding that the MIC value for *Candida albicans* was further reduced to a third with Ch-AgNPs compared to bare AgNPs is particularly intriguing. The larger zones of inhibition

observed in the disk diffusion assay corroborate the findings from the MIC determination, indicating that Ch-AgNPs possess stronger antimicrobial efficacy at lower concentrations. As seen in Table 3, Ch-AgNPs had the same MIC value as gentamicin used as a positive control for *Pseudomonas aeruginosa*. The study produced findings comparable to those outlined, indicating MIC values spanning from 10 μg/mL to 40 μg/mL for Ch-AgNPs against the examined Gram-positive and Gram-negative bacterial strains. This finding indicates that Ch-AgNPs effectively inhibited the growth of both types of bacteria within a relatively narrow concentration range (Farhadi et al., 2022).

Table 3. The MIC values for the AgNPs and Ch-AgNPs

Test microorganisms	MIC values (μg/mL)			
	AgNPs	**Ch-AgNPs**	**Gentamycine**	**Fluconazole**
Escherichia coli	3.75	1.86	3.75	-
Pseudomonas aeroginosa	1.86	0.94	0.94	-
Staphylococcus aureus	6.0	3.0	0.94	-
Enterococcus faecalis	0.94	0.48	3.75	-
Candida albicans	3.75	0.94	-	3.75

4. Conclusions

In our previous study, silver nanoparticles were synthesized by green synthesis method, optimized and characterized successfully for further use. In current study, the synthesis and characterization of both silver nanoparticles (AgNPs) and chitosan coated silver nanoparticles (Ch-AgNPs) have been successfully achieved by green synthesis method which is eco-friendly, simple and cheaper method. The integration of metal nanoparticles with biopolymers as Chitosan is becoming increasingly crucial for improving the safety profiles of formulations and assessing their biological activities. Through various analytical techniques such as UV-Vis spectroscopy, FTIR analysis, and X-ray diffraction, the formation, structure, and properties of these nanoparticles have been elucidated. Furthermore, biological activities of these nanoparticles have been explored, demonstrating promising potential in various biomedical applications. The results suggest that both AgNPs and Ch-AgNPs exhibit desirable properties for applications such as drug delivery, wound healing, and antimicrobial therapy. Further studies are warranted to fully understand their mechanisms of action and optimize their performance for specific biomedical applications. In conclusion, the synthesis, characterization, and biological activities of silver nanoparticles and chitosan nanoparticles represent a significant step forward in the development of advanced nanomaterials for biomedical applications especially with their safety profiles.

Statement of Conflict of Interest

The authors have declared no conflict of interest.

Author's Contributions

The contribution of the authors is equal.

References

Abedin MR., Umapathi S., Mahendrakar H., Laemthong T., Coleman H., Muchangi D., Santra S., Nath M., Barua S. Polymer coated gold-ferric oxide superparamagnetic nanoparticles for theranostic applications. Journal of Nanobiotechnology 2018; 16(1): 80.

Akter M., Sikde MT., Rahman MM., Ullah AKMA., Hossain KFB., Banik S., Hosokawa T., Saito T., Kurasaki M. A systematic review on silver nanoparticles-induced cytotoxicity: Physicochemical properties and perspectives. Journal of Advanced Research 2017; 9: 1-16.

Almeida EDP., Santos Silva LA., de Araujo GRS., Montalvão MM., Matos SS., da Cunha Gonsalves JKM., de Souza Nunes R., de Meneses CT., Oliveira Araujo RG., Sarmento VHV., Correa CB., Júnior JJ., Lira AAM. Chitosan-functionalized nanostructured lipid carriers containing chloroaluminum phthalocyanine for photodynamic therapy of skin cancer. European Journal of Pharmaceutics and Biopharmaceutics 2022; 179: 221-231.

Alomrani A., Badran M., Harisa GI. The use of chitosan-coated flexible liposomes as a remarkable carrier to enhance the antitumor. Saudi Pharmaceutical Journal 2019; 603-611.

Asif M., Yasmin R., Asif R., Ambreen A., Mustafa M., Umbreen S. Green synthesis of silver nanoparticles (AgNPs), structural characterization, and their antibacterial potential. Dose-response 2022; 20(1).

Ateş M., Yılmaz E., Kar B., Kars Durukan İ. Synthesis and characterization silver nanoparticles and coating with chitosan. Politeknik Dergisi 2021; 24(4): 1401-1408.

Azizi S., Namvar F., Mahdavi M., Ahmad MB., Mohamad R. Biosynthesis of silver nanoparticles using brown marine macroalga sargassum muticum aqueous extract. Materials 2013; 28788431.

Burdușel AC., Gherasim O., Grumezescu AM., Mogoantă L., Ficai A. Andronescu, E. Biomedical applications of silver nanoparticles: an up-to-date overview. Nanomaterials 2018; 8(9): 681.

Cinteza LO., Scomoroscenco C., Voicu SN., Nistor, CL., Nitu SG. Trica B., Jecu ML., Pectu C. Chitosan-stabilized Ag nanoparticles with superior biocompatibility and their synergistic antibacterial effect in mixtures with essential oils. Nanomaterials 2018; 8: 826.

Constantin M., Lupei M., Bucatariu SM., Pelin I M., Doroftei F., Ichi, DL., Daraba OM., Fundueanu G. PVA/chitosan thin films containing silver nanoparticles and ıbuprofen for the treatment of periodontal disease. Polymers 2022; 15(1): 4.

Desai N., Rana D., Salave S., Gupta R., Patel P., Karunakaran B., Sharma A., Giri J., Benival D., Kommineni N. Chitosan: a potential biopolymer in drug delivery and biomedical applications. Pharmaceutics 2023; 15(4): 1313.

Devaraj P., Kumari C., Renganathan A. Synthesis and characterization of silver nanoparticles using cannonball leaves and their cytotoxic activity against MCF-7 cell line. Journal of Nanotechnology 2013; 598328.

Di Martino A., Guselnikova OA., Trusova ME., Postnikov PS., Sedlarik V. Organic-inorganic hybrid nanoparticles controlled delivery system for anticancer drugs. International Journal of Pharmaceutics 2017; 526(1-2): 380–390.

Farhadi L., Mohtashami M., Saeidi J., Taheri G., Khojasteh-Taheri R., Rezagholizade-Shirvan A., Shamloo E., Ghasemi E. Green synthesis of chitosan-coated silver nanoparticle, characterization, antimicrobial activities, and cytotoxicity analysis in cancerous and normal cell lines. Journal of Inorganic and Organometallic Polymers and Materials 2022; 32: 1637-1649.

Giri AK., Jena B., Biswal B., Arun KP., Manoranjan A., Saumyaprava A., Laxmikanta A. Green synthesis and characterization of silver nanoparticles using Eugenia roxburghii DC. extract and activity against biofilm-producing bacteria. Science Reports 2022; 12: 8383.

Govindan S., Nivethaa EAK., Saravanan R. Synthesis and characterization of chitosan–silver nanocomposite. Applied Nanoscience 2012; 2: 299–303.

Ho BN., Pfeffer CM., Singh ATK. Update on nanotechnology-based drug delivery systems in cancer treatment. Anticancer Research 2017; 37(11): 5975–598.

Hou T., Guo Y., Han W., Zhou Y., Netala VR., Li H., Li H., Zhang Z. Exploring the biomedical applications of biosynthesized silver nanoparticles using perilla frutescens flavonoid extract: antibacterial, antioxidant, and cell toxicity properties against colon cancer cells. Molecules 2023; 28: 6431.

Hradılova S., Panacek A., Zborıl R. Green synthesized silver nanoparticles derived from an extract of the *Betula pendula* tree. Nanocon 2018; Czech Republic.

Huq MA., Ashrafudoulla M., Parvez MAK., Balusamy SR., Rahman MM., Kim JH., Akter S. Chitosan-coated polymeric silver and gold nanoparticles: biosynthesis, characterization and potential antibacterial applications: a review. Polymers 2022; 14(23): 5302.

Imran M., Ehrhardt CJ., Bertino MF., Shah MR., Yadavalli VK. Chitosan stabilized silver nanoparticles for the electrochemical detection of lipopolysaccharide: a facile biosensing approach for gram-negative bacteria. Micromachines 2020; 11: 413.

Jalab J., Abdelwahed W., Kitaz A., Al-Kayali R. Green synthesis of silver nanoparticles using aqueous extract of Acacia cyanophylla and its antibacterial activity. Heliyon 2021; 2405-8440.

Jeon IY., Baek JB. Nanocomposites derived from polymers and ınorganic nanoparticles. Materials 2010; 3(6): 3654–3674.

Jiménez-Gómez CP., Cecilia JA. Chitosan: a natural biopolymer with a wide and varied range of applications. Molecules 2020; 25(17): 3981.

Jyoti K., Baunthiyal M., Singh A. Characterization of silver nanoparticles synthesized using Urtica dioica Linn. leaves and their synergistic effects with antibiotics. Journal of Radiation Research and Applied Sciences 2016; 9: 217-227.

Kalaivani R., Maruthupandy M., Muneeswaran T. Synthesis of chitosan mediated silver nanoparticles (AgNPs) for potential antimicrobial applications. Frontiers in Laboratory Medicine 2018; 2: 30–35.

Khorrami S., Zarrabi A., Khaleghi M., Danaei M., Mozafari MR. Selective cytotoxicity of green synthesized silver nanoparticles against the MCF-7 tumor cell line and their enhanced antioxidant and antimicrobial properties. International Journal of Nanomedicine 2018; 13: 8013-8024.

Komsthöft T., Bovone G., Bernhard S., Tibbitt MW. Polymer functionalization of inorganic nanoparticles for biomedical applications. Current Opinion in Chemical Engineering 2022; 37: 100849.

Liao C., Li Y., Tjong SC. Bactericidal and cytotoxic properties of silver nanoparticles. International Journal of Molecular Sciences 2019; 20(2): 449.

Liu C., Zhu Y., Lun X., Sheng H., Yan A. Effects of wound dressing based on the combination of silver@curcumin nanoparticles and electrospun chitosan nanofibers on wound healing. Bioengineered 2022; 13(2): 4328–4339.

Malik S., Muhammad K., Waheed Y. Emerging applications of nanotechnology in healthcare and medicine. Molecules 2023; 28(18): 6624.

Mallikarjuna K., Narasimha G., Dillip GR., Praveen B., Shreedhar B., Sreelakshmi C., Reddy BPD. Green synthesis of silver nanoparticles using Ocimum leaf extract and their characterization. Digest Journal of Nanomaterials and Biostructures 2011; 6: 181–186.

Maslamani N., Khan SB., Danish EY., Bakhsh EM., Akhtar K., Asiri AM. Metal nanoparticles supported chitosan coated carboxymethyl cellulose beads as a catalyst for the selective removal of 4-nitrophenol. Chemosphere 2022; 291(3): 133010.

Mikhailova EO. Silver nanoparticles: mechanism of action and probable bio-application. Journal of Functional Biomaterials 2020; 11(4): 84.

Nate Z., Moloto MJ., Mubiayi PK. Green synthesis of chitosan capped silver nanoparticles and their antimicrobial activity. MRS Advances 2018; 3: 2505-2517.

Ozcelik B., Kara A. Evaluation of biological activities of silver nanoparticles (AgNPs) synthesized by green nanotechnology from birch (Betula spp.) branches extract. Turkish Journal of Analytical Chemistry 2023; 5(2): 151-161.

Panja S., Chaudhuri I., Khanra K., Bhattacharyya N. Biological application of green silver nanoparticle synthesized from leaf extract of Rauvolfi serpentina Benth. Asian Pacific Journal of Tropical Disease 2016; 6(7): 549-556.

Rathod D., Golinska P., Wypij M., Dahm H., Rai M. A new report of Nocardiopsis valliformis strain OT1 from alkaline Lonar crater of India and its use in synthesis of silver nanoparticles with special reference to evaluation of antibacterial activity and cytotoxicity. Medical Microbiology and Immunology 2016; 205: 435-447.

Rautela A., Rani J., Debnath M. Green synthesis of silver nanoparticles from Tectona grandis seeds extract: characterization and mechanism of antimicrobial action on different microorganisms. Journal of Analytical Science and Technology 2019; 10(5).

Raza S., Ansari A., Siddiqui NN., Ibrahim F., Abro MI., Aman A. Biosynthesis of silver nanoparticles for the fabrication of non-cytotoxic and antibacterial metallic polymer based nanocomposite system. Science Reports 2021; 11: 10500.

Saeidi J., Motaghipur R., Sepehrian A., Mohtashami M., Forooghi Nia F., Ghasemi A. Dietary fats promote inflammation in Wistar rats as well as induce proliferation, invasion of SKOV3 ovarian cancer cells. Journal of Food Biochemistry 2020; 44(5): 13177.

Saxena M., Saxena J., Nema R., Kurmukov AG. Phytochemistry of medicinal plants. Journal of Pharmacognosy and Phytochemistry 2013; 1:168–182.

Shinde S., Folliero V., Chianese A., Zannella C., De Filippis A., Rosati L., Prisco M., Falanga A., Mali A., Galdiero M. Synthesis of chitosan-coated silver nanoparticle bioconjugates and their antimicrobial activity against multidrug-resistant bacteria. Applied Science. 2021; 11: 9340.

Souza TGF., Ciminelli VST., Mohallem NDS. A comparison of TEM and DLS methods to characterize size distribution of ceramic nanoparticles. Journal of Physics: Conference Series 2016, Bento Gonçalves, Brazil.

Takáč P., Michalková R., Čižmáriková M., Bedlovičová Z., Balážová Ľ., Takáčová G. The Role of silver nanoparticles in the diagnosis and treatment of cancer: are there any perspectives for the future?. Life 2023; 13: 466.

Wang L., Du L., Wang M. Chitosan for constructing stable polymer-inorganic suspensions and multifunctional membranes for wound healing. Carbohydrate Polymers 2022; 285: 119209.

Wulandari IO., Pebriatin BE., Valiana V., Hadisaputra S., Ananto AD., Sabarudin A. Green synthesis of silver nanoparticles coated by water soluble chitosan and its potency as non-alcoholic hand sanitizer formulation. Materials 2022; 15(13): 4641.

Yan D., Li Y., Liu Y., Li N., Zhang X., Yan C. Antimicrobial properties of chitosan and chitosan derivatives in the treatment of enteric infections. Molecules 2021; 26 (23): 7136.

Zentel R. Polymer coated semiconducting nanoparticles for hybrid materials. Inorganics 2020; 8(3).